

# Catalysis Science & Technology

Accepted Manuscript



This is an *Accepted Manuscript*, which has been through the Royal Society of Chemistry peer review process and has been accepted for publication.

*Accepted Manuscripts* are published online shortly after acceptance, before technical editing, formatting and proof reading. Using this free service, authors can make their results available to the community, in citable form, before we publish the edited article. We will replace this *Accepted Manuscript* with the edited and formatted *Advance Article* as soon as it is available.

You can find more information about *Accepted Manuscripts* in the [Information for Authors](#).

Please note that technical editing may introduce minor changes to the text and/or graphics, which may alter content. The journal's standard [Terms & Conditions](#) and the [Ethical guidelines](#) still apply. In no event shall the Royal Society of Chemistry be held responsible for any errors or omissions in this *Accepted Manuscript* or any consequences arising from the use of any information it contains.

**The Graphitic Carbon Strengthened Synergetic Effect between Pt and FeNi for  
CO Preferential Oxidation in Excess Hydrogen at Low Temperature**

Limin Chen<sup>a,b\*</sup>, Yunfeng Bao<sup>a</sup>, Yuhai Sun<sup>a</sup>, Ding Ma<sup>b,c</sup>, Daiqi Ye<sup>a</sup>, Bichun Huang<sup>a</sup>

<sup>a</sup>Guangdong Provincial Key Laboratory of Atmospheric Environment and Pollution Control, School of Environment and Energy, South China University of Technology, Guangzhou 510006, China

<sup>b</sup>State Key Laboratory of Catalysis, Dalian Institute of Chemical Physics, Chinese Academy of Sciences, Dalian 116023, China

<sup>c</sup>College of Chemistry and Molecular Engineering, Peking University, Beijing 100871, China

---

\*Corresponding author. E-mail: [liminchen@scut.edu.cn](mailto:liminchen@scut.edu.cn); Tel.: +86-20-39380516.

**ABSTRACT**

A variety of carbon materials supported PtFeNi catalysts have been prepared and tested for CO preferential oxidation (PROX) in excess hydrogen. 100% O<sub>2</sub> and CO conversions have been achieved over carbon black (CB) and carbon nanotubes (CNTs) supported PtFeNi catalysts at room temperature in feed gas containing 1% CO, 0.5% O<sub>2</sub> (volume ratio) and H<sub>2</sub> balance gas. N<sub>2</sub> adsorption, temperature-programmed desorption (TPD) and transmission electron microscopy (TEM) studies indicate that the carbon textural properties and surface chemistry determine the catalyst particle size distribution and mean size; but the mean particle size is not essential to the catalytic performances within the investigated particle size range. X-ray diffraction (XRD), resistance measurements and the designed catalytic reaction results reveal that the ability of graphitic carbon to capture and shuttle electrons from noble metal to spatially different site FeNi species through the  $\pi$ - $\pi$  network, enable the indirect interactions between Pt and FeNi species, leading to the strengthened synergistic effect, enhancing CO oxidation activity at room temperature, increasing Pt utilization efficiency, apparently decreasing Pt loading level.

**Keywords:** Indirect interactions, Synergetic effect, Low Pt loading, CO preferential oxidation (PROX), High Catalytic Performance

## 1. Introduction

Proton exchange membrane fuel cells (PEMFCs) has been considered to be one of the most promising candidates to replace conventional fossil fuels, due to its high energy efficiency, environment-friendly characteristics and low operating temperature [1-2]. However, most commercial fuel of hydrogen is generally produced through various hydrocarbons or bio-alcohols, from fossil fuels or biomass, via the steam reforming and water-gas shift (WGS) reactions. The resultant H<sub>2</sub>-rich gases generally contain 0.5 - 1.0 vol. % of CO due to the thermodynamic limitation of WGS reaction [1-22]. Unfortunately, small amount of CO severely poisons the anode catalyst of the PEMFCs, therefore, purifying CO to ppm level is required prior to the introduction of hydrogen to PEMFCs [1-22]. Among the various methods investigated, low temperature preferential oxidation of CO in excess H<sub>2</sub> streams (PROX) is presently regarded as one of the most promising and cost-effective way [1-22].

Among the various catalysts, Pt-based catalysts especially Fe [5-8,20-21], Co [9-14], Ni [14-19,21], Cu [11,22] and Ag [23] etc. promoted Pt catalysts are the most promising candidates. However, it is extremely difficult to realize total conversion of CO at ambient temperatures with reasonable cost, which is particularly important for fuel cell applications in transportation [10,13,17,20]. To the best of our knowledge, among all the supported Pt catalysts reported in the literature, there are only a few supported Pt catalysts can accomplish total conversion of CO at room temperature or even lower [4,5,21], mainly including our PtFe/SiO<sub>2</sub> [5] and later developed PtFeNi/CNTs [21] catalysts.

In order to find effective, low-cost and highly robust Pt-based catalysts, besides the promotion effects of promoters, the effects of various supports on the catalytic performance have been extensively investigated in the promotion catalytic system, including CeO<sub>2</sub> [11], TiO<sub>2</sub> [12,14], SiO<sub>2</sub> [4,5,14], Al<sub>2</sub>O<sub>3</sub> [8,11,22], zeolites [10] and carbon materials [6,9,13-21] etc.. The results indicated that some supports could help to distribute the active component uniformly [17], some could interact with the active

component [24] or influence the chemical state of the active component [12]. Especially, Petkov et al. reported the role of support-nanoalloy interactions on CO oxidation [14]. Their investigation indicated that by controlled thermo-chemical treatment, oxygen activation sites on TiO<sub>2</sub> supported nanoalloy could be provided both by the second/third metal sites in the nanoalloy (Type-I site) and by the anionic oxygen deficiency sites located at the nanoalloy-support perimeter zone (Type-II site). However, only Type-I site can be achieved for the nanoalloys on carbon support; neither can be generated on SiO<sub>2</sub> supported nanoalloy, resulting in the lowest activity for the silica-supported nanoalloys.

Petkov's research is based on the assumption that the promotion effects of base transition metals originates from the Pt-nanoalloy. However, our extensive investigation demonstrated that the coordinatively unsaturated transition metal cations confined in nanosized Pt matrices were the main oxygen-activation sites [5-7,9,21]. Therefore, Petkov's discovery could not explain the extremely high activity of SiO<sub>2</sub> and carbon materials supported PtM (M = Fe, Ni, Co) catalysts for CO PROX and CO oxidation [5-7,9,13,21]. Our previous research indicates that 3 wt%PtFeNi/CNTs catalyst is extremely highly active, which can almost totally remove CO in the gas composition of 1 vol% CO, 0.5vol% O<sub>2</sub> and H<sub>2</sub> balance even at 6 °C [21]. Compared with other highly active catalysts [5,6,9,13], this catalyst consists of evidently lower Pt loading level, operating with stoichiometric O<sub>2</sub>, much higher concentration of H<sub>2</sub> and nearly the same gas hourly space velocity. Our further investigation indicates that in-situ formed coordinatively unsaturated FeO<sub>x</sub> and/or NiO<sub>x</sub> species confined in Pt matrices are active species and over oxidation of Fe and Pt species deactivates the catalysts seriously [21]. These discoveries are similar to our previously reported PtFe/SiO<sub>2</sub> catalysts [5]; then, what reasons results in the extremely high activity of PtFeNi/CNTs even with apparently lower Pt loadings? Is it from the unique properties of CNTs or the general properties of carbon?

Recently, the ability of carbon nanotubes and graphene-based systems to capture

and shuttle electrons through the  $\pi$ - $\pi$  network has been confirmed through spectroscopic studies [25-26]. This feature enables incorporate a semiconductor and Pt nanoparticle particles on a single graphene or reduced graphene oxide sheet, and then the multifunctional photocatalyst has been demonstrated for photocatalytic H<sub>2</sub> production [27-28]. This photocatalyst can carry out selective catalytic processes at separate sites and tune the selectivity and efficiency of photo-catalytic reduction and oxidation processes, independently. As far as our highly active PtFeNi/CNTs catalyst, do CNTs possess the ability to capture electron and shuttle them, and will this ability contribute to the high catalytic activity or not?

In order to answer the above questions and reveal the origin of extremely highly active PtFeNi/CNTs catalyst compared with PtFe/SiO<sub>2</sub> and other catalysts, four types of carbon, CNTs, carbon black (CB) with high graphitization, oxidized carbon black (CB-o), activated carbon (AC) with less graphitization, were used to prepare PtFeNi catalysts and their catalytic properties for CO PROX were tested. CB can be utilized to exclude the unique properties of CNTs, for instance, confinement effects; CB-o can be used to investigate the negative effects of carbon surface oxidation on the ability of carbon to capture electrons and shuttle them; AC can facilitate to deliberate the roles of graphitization degree and the well-developed pore structure on the catalytic performance. Therefore, the properties on catalytic performance were investigated through N<sub>2</sub> adsorption, TPD, TEM, XRD and resistance measurements. The discovery of this research will further direct us to design and prepare more effective, economical and robust catalysts for CO PROX in H<sub>2</sub> rich stream.

## 2. Experimental

### 2.1. Materials

Multi-walled carbon nanotubes with 4~8 nm i.d. and 10~20 nm o.d. were purchased from Chengdu Organic Chemicals Co., Ltd., China, which contained 0.41 wt.%Fe and 0.35 wt.%Ni, denoted as CNTs(FeNi). CNTs(FeNi) purification was

conducted by a procedure from the literature [21], and the obtained sample was labeled as CNTs-p. Carbon black was purchased from Acros, marked as CB. CB was oxidized in 5% O<sub>2</sub> balanced in He (volume ratio) at 600 °C for 3 h, and the obtained material was denoted as CB-o. Commercial granulated activated carbon (sieved into 40-60 mesh) was obtained from Beijing Guanghai Woods Ltd., Beijing, China. The carbon was washed with boiling aqueous nitric acid (0.001 N) and dried at 120 °C overnight. Then, the sample was further treated in He at 600 °C for 3 h and the obtained sample was denoted as AC.

## 2.2. Catalyst preparation

Pt catalysts were prepared by conventional wetness impregnation method at room temperature using ethanol solution of hexachloroplatinic acid (Shenyang Chemical Reagent Company, AR) according to the metal loading. The samples were further dried at 120 °C for 12 h. The Fe and Ni promoted catalysts were prepared by the sequential wetness impregnation method. For example, FeNi(H500)Pt catalyst, carbon support was first impregnated with ethanol solution of ferric nitrate and nickel nitrate mixture followed by drying at 120 °C for 12 h then pretreated in H<sub>2</sub> at 500 °C for 2 h, and finally impregnated with ethanol solution of hexachloroplatinic acid. For all PtFeNi catalysts, the loading of Pt, Fe and Ni were 3, 0.41 and 0.35 wt.% (atomic ratio, 15:7:6), respectively; for PtFe and PtNi catalysts, the loading of Fe and Ni were 0.75 and 0.81 wt% (the same atomic ratio, 15:13), respectively. The catalysts were pretreated in H<sub>2</sub> at 500 °C for 2 h before catalytic tests.

## 2.3. Catalytic reaction test

The catalytic reaction tests were performed in a fixed bed flow reactor. A small quartz tube containing a thermocouple was placed in the middle of the catalyst bed. Generally, 60 mg of catalyst sample was used. A gas mixture containing 1% CO and 0.5% O<sub>2</sub> (volume ratio) in H<sub>2</sub> was fed at a flow rate of 25 ml/min, with gas hourly space velocity 25 000 ml/g·h. The composition of the effluent gas was monitored

on-line with a gas chromatograph (Agilent Technologies GC-6890N) equipped with PN and TDX-01 columns. The CO conversion was calculated from the change in CO concentration, and selectivity towards CO<sub>2</sub> was obtained from the O<sub>2</sub> mass balance. The details were elaborated in our previous publications [29-30].

#### 2.4. Characterization

The texture properties of carbon supports were determined by N<sub>2</sub> adsorption-desorption isotherms at 77 K using an AS-1-MP adsorption instrument. Samples were degassed at 383 K overnight before the measurements [29]. The specific surface areas were calculated using the BET equation, and the t-plot method was used to calculate the micropore volumes and areas [29]. The temperature-programmed desorption (TPD) experiments were carried out in a quartz U type microreactor, connected with an on-line quadruple mass spectrometer (Balzers, OmniStar GSD300 O). The samples (60 mg) were first flushed with He (30 ml/min) at room temperature for 2 h. Subsequently, the temperature was increased to 990 °C at a rate of 5 °C/min. MS intensities for 2 (H<sub>2</sub>), 4 (He), 28 (CO), and 44 (CO<sub>2</sub>) were measured as a function of temperature.

Transmission electron microscopy (TEM, TECNAI Spirit) was used to study the size of metal particles. XRD measurements were carried out on a Rigaku D/Max 2500 diffractometer with a Cu ka monochromatized radiation source at 40 kV and 250 mA. The sheet resistivities were measured by a conventional SZ-82 four-probe instrument (Suzhou Tel. Apparatus Co., China).

### 3. Results and discussion

#### 3.1. Reaction results

##### 3.1.1. The catalytic performance of different carbon supported Pt catalysts

Fig. 1 presents the variation of O<sub>2</sub> conversion (A), CO conversion (B) and

selectivity (C) over different carbon supported 3 wt.% Pt catalysts as a function of reaction temperature. Pt/CNTs-p exhibited the highest catalytic activity with the highest O<sub>2</sub> and CO conversions among the studied catalysts. For example, O<sub>2</sub> and CO conversions were 35.7% and 37.1% at 23 °C, respectively. At around 125 °C, O<sub>2</sub> was completely consumed and CO conversion reached the maximum of 77.8% on Pt/CNTs-p sample. The other three catalysts (supported over CB, CB-o, AC) showed very low reactivity below 120 °C. The full O<sub>2</sub> conversion was obtained at 200 °C over Pt/CB catalyst and the corresponding maximum CO conversion was 66.6%. For Pt/CB-o catalyst, the full O<sub>2</sub> conversion was obtained at 240 °C and the corresponding maximum CO conversion was 56.7%. For Pt/AC catalyst, the full O<sub>2</sub> conversion was obtained at 210 °C and the corresponding maximum CO conversion was only 51.2%. The O<sub>2</sub> reactivity of the four catalysts followed the order of Pt/CNTs-p > Pt/CB > Pt/AC > Pt/CB-o, whereas the maximum CO conversion decrease followed the order of Pt/CNTs-p > Pt/CB > Pt/CB-o > Pt/AC.

### 3.1.2. The catalytic performance of different carbon supported Pt-based catalysts

Fig. 2 presents O<sub>2</sub> conversion (A), CO conversion (B) and selectivity (C) over different carbon supported Fe and Ni promoted Pt catalysts at 23 °C after reaction for certain time. Since PtFeNi/CNTs-p catalyst after activation at 500 °C in H<sub>2</sub> can nearly completely remove CO at 6 °C in feed gas containing 1% CO, 0.5% O<sub>2</sub> (volume ratio) and H<sub>2</sub> balance [21]; H<sub>2</sub> oxidation occurs at temperature higher than 6 °C and the produced water displays apparently promotion effects. Therefore, in order to compare the catalytic performance at the same reaction temperature, Pt/CNTs(FeNi), PtFeNi/CB, PtFeNi/CB-o and PtFeNi/AC catalysts were selected. All of the catalysts lost activities to some extent, but their selectivity to CO oxidation did not decrease. Pt/CNTs(FeNi) and PtFeNi/CB catalysts had better catalytic reactivity and stability, especially for Pt/CNTs(FeNi) catalyst, both of them showed nearly complete O<sub>2</sub> conversion and CO conversion at 23 °C. PtFeNi/CB-o and PtFeNi/AC catalysts lost activities very quickly. Furthermore, PtFeNi/AC exhibited the worst reactivity and

stability, which only displayed 40% and 30% initial O<sub>2</sub> and CO conversions at 23 °C, respectively. The initial catalytic activity decreased in the following order: Pt/CNTs(FeNi) ≥ PtFeNi/CB > PtFeNi/CB-o > PtFeNi/AC.

These results indicate that the addition of Fe and Ni can dramatically enhance the catalytic activity of Pt catalysts; besides, the catalysts can be deactivated at some extent, which have been extensively investigated in our previous publications [5,21]. In addition, carbon supports also play important roles on the catalytic performance. On one hand the same PtFeNi catalysts with different carbon support exhibited different catalytic performances; on the other hand, the same carbon supported Pt and PtFeNi catalysts gave different catalytic activity trends. For example, Pt/AC catalyst presented significantly higher activity (O<sub>2</sub> conversion at the same temperature) than that of Pt/CB-o; on the contrary, PtFeNi/AC catalyst showed significantly lower activity (O<sub>2</sub> conversion at 23 °C) than that of PtFeNi/CB-o. Besides, it is interesting that all PtFeNi catalysts exhibit stable selectivity although O<sub>2</sub> and CO reactivity show some extent loss. In order to elucidate the roles of carbon supports on the catalytic performances, the catalysts have been investigated by a number of characterization methods (vide infra).

### 3.2. Characterization results

#### 3.2. 1. Textural properties and surface chemistry of carbon supports

The nitrogen adsorption/desorption isotherms of different carbon supports are demonstrated in Supporting Information (Fig. S1) and the corresponding textural parameters were listed in Table 1. The isotherm profile of AC is typical IV type with rich micropores and mesopores; the calculated specific surface area and mean pore diameter (MPD) are 1158.0 m<sup>2</sup>/g and 2.1 nm, respectively. The isotherm profile of CB-o is similar to AC but has much more mesopores and less micropores. For CB-o, the calculated specific surface area and MPD are 210.2 m<sup>2</sup>/g and 11.2 nm, respectively. In comparison with CB-o, CB has much less mesopores and micropores and the

corresponding specific surface area and MPD are 75.8 m<sup>2</sup>/g and 6.5 nm, respectively. For CNTs, the calculated specific surface area and inner pore size are 172.2 m<sup>2</sup>/g and 4 - 8 nm, respectively.

Temperature-programmed desorption (TPD) in an inert gas (He, Ar, N<sub>2</sub>) are effective in determining different oxygen-containing groups of carbon materials [29, 30-34]. The TPD curves of CO and CO<sub>2</sub> from different carbon supports are shown in Supporting Information (Fig. S2) and the corresponding integration area of CO and CO<sub>2</sub> desorption from TPD is listed in Table 1. It is clear that AC has much more acidic oxygen containing functional groups, CB-o possess moderate amount of oxygen containing functional groups, CNTs holds less oxygen containing functional groups compared with CB-o and AC, and CB hardly bears any oxygen containing functional groups.

### 3.2. 2. Particle size of different carbon supported PtFeNi catalysts

Fig. 3 presents transmission electron microscopy (TEM) images and the corresponding particle size distributions of different carbon supported PtFeNi catalysts after activation in H<sub>2</sub> at 500 °C for 2 h. The PtFeNi particle size distribution on AC (1.5 - 6 nm) is a little broader than that on the other three supports. The average particle size of PtFeNi/AC catalyst is about 3.7 nm, which is much bigger than that of others. The particle size distribution of PtFeNi/CB-o catalyst is very narrow with an average particle size of 1.6 nm. PtFeNi/CB catalyst mainly consists of particles with diameter from 2 to 3 nm, giving average particle size about 2.5 nm. Pt/CNTs(FeNi) catalyst exhibits very narrow particle size distribution, giving average particle size about 1.6 nm. The average particle size of the four catalysts decreased in the following order: PtFeNi/AC > PtFeNi/CB > PtFeNi/CB-o ≈ Pt/CNTs(FeNi).

### 3.3. Discussions

#### 3.3.1. The relationship between catalyst particle size and catalytic performance

It has been well established that the textural properties and surface chemistry of carbon play vital roles on the catalyst particle size [29,30,34]. Large amounts of mesopore tend to increase the dispersions of catalyst particles, instead, negative effect of microporous structure on the dispersions of catalyst particles; rich surface functional groups not only make size distribution of catalyst particles bimodal, but also promote the formation of very fine metal particles. This is in good agreement with our previous study [30]. In most cases, the particle size is crucial to the catalytic performances [29, 34]. The mean particle sizes and catalytic activities of PtFeNi catalysts at 23 °C as a function of different carbons are displayed in Fig. 4. It is clear that PtFeNi/CB-o and Pt/CNTs(FeNi) catalysts possess similar mean particle size but present quite different CO conversion at 23 °C. On the contrary, PtFeNi/CB catalyst has apparently bigger mean particle size than that of Pt/CNTs(FeNi) but with comparable O<sub>2</sub> and CO conversion. This means the mean particle size is not the only factor to govern the catalytic performances and there should be other factors, other than textural properties and surface chemistry of carbon, to determine the catalytic performances.

### 3.3.2. The graphitic carbon strengthened synergetic effect between Pt and FeNi

As discussed above, the particle size is not crucial to the catalytic performance within the investigated particle size range. Inspired by the multifunctional photocatalyst with spatially separate active components on a graphene sheet [27-28], the authors bring up that the graphitic carbon may tune the interactions between Pt and FeNi, strengthening the synergetic effect and causing the extremely high catalytic performance. In order to confirm and complete this bold assumption, the ability of carbon to capture and shuttle electrons through the  $\pi$ - $\pi$  network (the graphitization degree, conductivity) and their abilities on the catalytic properties have been investigated in details below.

The graphitization degree of carbon materials can be reflected by XRD characterization, as shown in Fig. 5. The diffraction peaks at 25.78, 42.88, 53.58 and

78.18° are characteristics of graphic carbon (JCPDS 656212). The strong and sharp diffraction peaks in CNTs verify the high graphitization degree of CNTs sample, which are essentially composed of coaxial graphitic cylinders. CB and CB-o show similar but slightly broadened diffraction peaks with slightly lower intensity compared to CNTs. In comparison, the diffraction peaks of AC is broadened obviously (Fig. 5d), indicating evidently poor crystallized graphitic structure. Generally, the high graphitization degree means complete  $\pi$ - $\pi$  network, indicating free movement of delocalized  $\pi$ -electrons on carbon surface, i.e. the high electrical conductivity of carbon materials [35]. As far as CB-o, it displays similar diffraction feature to CB; however, it bears more surface functional groups, suppress the movement of  $\pi$ -electrons, resulting in lower electrical conductivity. Therefore, the conductivity of the carbon materials was measured according to the resistivity measurement, as shown in Fig. 6. The resistivities of CNTs, CB, CB-o and AC are 0.04, 0.45, 1.35 and 141.80  $\Omega\cdot\text{cm}$ , respectively; which implies that the electron conductivity decreases in the order: CNTs > CB > CB-o > AC.

As mentioned in the Introduction section, the carbon with graphitic structure can capture and shuttle electrons to different sites through  $\pi$ - $\pi$  network. Furthermore, recent spectroscopic studies have proved the ability of graphene oxide to accept electrons from excited semiconductor nanoparticles and then reduce  $\text{Ag}^+$  at another site spatially different from the semiconductor nanoparticles [25]. Based on this observation, Pt-loaded graphene- $\text{Sr}_2\text{Ta}_2\text{O}_7\text{-xN}_x$  multifunctional photocatalyst with selective catalytic processes at separate sites has been successfully demonstrated [27]. Our previous research demonstrated that coordinatively unsaturated  $\text{FeO}_x$  and/or  $\text{NiO}_x$  confined in nanosized Pt matrices are active species for PROX of CO and there are interactions between Pt and  $\text{FeO}_x/\text{NiO}_y$  species [5-7,21]. All investigations suggest the ability of graphitic carbon to capture electrons and shuttle them to spatially different sites through  $\pi$ - $\pi$  network may tune the interactions between spatially separate Pt and  $\text{FeO}_x/\text{NiO}_y$  species, i.e. indirect interaction between Pt and  $\text{FeO}_x/\text{NiO}_y$  species. This speculation means the higher conductivity of the carbon materials, the stronger the

indirect interaction is. Furthermore, this indirect interaction between Pt and  $\text{FeO}_x/\text{NiO}_y$  species may weaken CO adsorption on Pt and facilitate the oxygen adsorption, enhancing CO oxidation activity. On the other hand, this indirect interaction may also enable optimum CO adsorption and  $\text{O}_2$  adsorption on Pt and  $\text{FeO}_x/\text{NiO}_y$  species, respectively; then CO oxidation reaction can be proceeded through chemical reaction-diffusion wave, as proposed in the previous publications [23,36]. There are also other possibilities, such as metal modified carbon catalyzed CO PROX reaction, extensively studied in electro-catalysis recently [37-39]. Either way will enhance Pt utilization efficiency, leading to better or similar catalytic performances with relatively low Pt loadings. This concept is illustrated in Fig. 7 in details.

In order to verify the above concept, the relationship between the conductivity and the catalytic performance was investigated, as shown in Fig. 6. It is interesting that the electron conductivity of carbon materials agrees very well with the catalytic activities of the corresponding catalysts, which can be seen from the plots of CO and  $\text{O}_2$  conversions. PtFeNi catalysts supported on the highly electronic conductive supports, such as CNTs, CB and CB-o, exhibit high CO conversions; however, when supported on the low electronic conductive supports, such as AC, it displays low catalytic activities. Besides the high CO oxidation activity of PtFeNi catalysts, the deactivation rate of different carbon supported catalysts follows the order  $\text{AC} > \text{CB-o} > \text{CB} > \text{CNTs}$ . The results indicated that both CO oxidation activity and stability agree well with the electronic conductivity of the carbon support. This implies that the strong indirect interactions may benefit to the good catalytic performance. This observation confirms that the graphitic carbon strengthens the synergetic effect between Pt and FeNi, leading to high catalytic performance with low Pt loading level.

It is well known that the X-ray photoelectron spectroscopy (XPS) is a good way to characterize the interactions between metal-supports and/or metal-promoters.

Therefore, XPS characterization was conducted. However, there is very low signal for Fe 2p and Ni 2p due to their low loading level. Generally, different catalyst preparation method will also influence the metal-support interactions; sometimes even change the structure of active phase. Then, different catalyst preparation methods have been designed to adjust the graphitic carbon induced indirect interactions to investigate its effects on the catalytic performance.

Fig. 8 compared the catalytic performance of CB supported FeNi promoted Pt catalysts with different preparation methods. FeNi(H500)Pt catalyst exhibits apparent higher catalytic activity and stability compared with FeNiPt and PtFeNi catalysts. Before impregnated with platinum precursor, FeNi/CB was pre-reduced with H<sub>2</sub> which will produce element iron/nickel and obtain stronger metal-carbon interactions simultaneously. When impregnated with platinum precursor, the nucleation is prone to occur around FeNi particles, which is helpful to create active species (shorten distance between Pt and FeNi nanoparticles). Therefore, this preparation method contributes to stronger indirect interactions, resulting in better catalytic performance. This example verifies that the graphitic carbon induced indirect interactions between Pt and FeNi species plays important roles on the synergistic effects. And the catalytic performance difference between CNTs and CB supported PtFeNi may be due to the unique properties of CNTs.

In order to further prove the important roles of the graphitic carbon induced indirect interactions on the synergistic effects, the highly conductive flake graphite (FG) supported Pt and FeNi catalysts was physically mixed by grinding to prepare PtFeNi/FG catalyst and their catalytic properties for CO PROX were evaluated as shown in Supporting Information (Fig. S3). This series of catalyst can effectively exclude the interfacial effects of Pt-FeNi and alloying effects of PtFeNi on the performances; and the promotion effects should come from the graphitic carbon induced indirect interactions if exist. It is very interesting that both CO and O<sub>2</sub> conversions are enhanced sharply compared with Pt/FG and FeNi/FG catalysts, as

shown in Fig. S3. This is a good example to confirm the significant roles of the graphitic carbon induced indirect interactions on the synergistic effects.

Thus, carbon materials with graphitic structure can capture electrons and shuttle them to spatially different sites, which induces indirect interactions between Pt and FeNi species, consolidating the synergistic effect, leading to high catalytic activity of PtFeNi/CNTs catalysts with much lower Pt loadings. The roles of the graphitic carbon induced indirect interactions between Pt and transition metal species on thermal catalytic processes have rarely been recognized, although it is well understood in the electrochemical activity and durability of the fuel cell catalytic layers. This discovery may pave the way to further reduce the loading level of noble metal and search for more optimal and economical catalysts for CO PROX reaction and other thermal catalytic processes.

#### 4. Conclusions

CNTs, CB, CB-o and AC have been selected to load PtFeNi catalysts and their catalytic properties for PROX of CO reaction were evaluated. Through the comparative study, it is found that the ability of graphitic carbon to capture electrons and shuttle them to different sites induces the indirect interactions between Pt and FeNi species, strengthening the synergistic effect. This graphitic carbon amplified synergistic effect leads to the extremely high catalytic activity with much lower Pt loadings, when operating with stoichiometric O<sub>2</sub>, much higher concentration of H<sub>2</sub> and nearly the same gas hourly space velocity. This discovery will help to design more effective, economical and robust catalysts for CO PROX reaction and other thermal catalytic processes.

#### Acknowledgments

The authors gratefully thank Dr. Prof. Xinhe Bao and Dr. Prof. Xiulian Pan at Dalian Institute of Chemical Physics, Chinese Academy of Sciences, for their enthusiastic supervision and helpful discussions. This work is financially supported

by the National Natural Science Foundation of China (21207039, 51108187), the Fundamental Research Funds for the Central Universities (Grant No. 2015zz052) and Guangdong Natural Science Foundation, China (Grant No. S2011010000737).

## References

- 1 E. D. Park, D. Lee and H. C. Lee, *Catal. Today*, 2009, 139, 280.
- 2 K. Liu, A. Q. Wang and T. Zhang, *ACS Catal.* 2012, 2, 1165.
- 3 B. T. Qiao, A. Q. Wang, L. Li, Q. Q. Lin, H. S. Wei, J. Y. Liu and T. Zhang, *ACS Catal.*, 2014, 4, 2113.
- 4 S. Huang, K. Hara, Y. Okubo, M. Yanagi, H. Nambu and A. Fukuoka, *Appl. Catal., A*, 2009, 365, 268.
- 5 Q. Fu, W. X. Li, Y. X. Yao, H. Y. Liu, H. Y. Su, D. Ma, X. K. Gu, L. M. Chen, Z. Wang, H. Zhang, B. Wang and X.H. Bao, *Science*, 2010, 328, 1141.
- 6 H. Xu, Q. Fu, Y. X. Yao and X. H. Bao, *Energy Environ. Sci.*, 2012, 5, 6313.
- 7 X. G. Guo, Q. Fu, Y. X. Ning, M. M. Wei, M. R. Li, S. Zhang, Z. Jiang and X. H. Bao, *J. Am. Chem. Soc.* 2012, 134, 12350.
- 8 A. Tomita, K. Shimizu, K. Kato and Y. Tai, *Catal. Commun.* 2012, 17, 194.
- 9 H. Xu, Q. Fu, X. G. Guo and X. H. Bao, *ChemCatChem* 2012, 4, 1645.
- 10 C. X. Wang, L. H. Zhang, Y. T. Liu, *Appl. Catal., B*, 2013, 136, 48.
- 11 J. Kugai, T. Moriya, S. Seino, T. Nakagawa, Y. Ohkubo, H. Nitani and T. A. Yamamoto, *Int. J. Hydrogen Energy*, 2013, 38, 4456.
- 12 H. R. Zheng, H. Y. Yang, R. R. Si, W. X. Dai, X. Chen, X. X. Wang, P. Liu and X. Z. Fu, *Appl. Catal., B*, 2011, 105, 243.
- 13 C. Wang, B. D. Li, H. Q. Lin and Y. Z. Yuan, *J. Power Sources*, 2012, 202, 200.
- 14 L. Yang, S. Y. Shan, R. Loukrakpam, V. Petkov, Y. R. Bridgid, N. Wanjala, M. H. Engelhard, J. Luo, J. Yin, Y. S. Chen and C. J. Zhong, *J. Am. Chem. Soc.*, 2012, 134, 15048.
- 15 K. Tanaka, M. Shou and Y. Z. Yuan, *J. Phys. Chem. C*, 2010, 114, 16917.
- 16 H. W. Yang, C. Wang, B. D. Li, H. Q. Lin, K. Tanaka and Y. Z. Yuan, *Appl. Catal., A*, 2011, 402, 168.
- 17 S. H. Lu, C. Zhang and Y. Liu, *Int. J. Hydrogen Energy*, 2011, 36, 1939.
- 18 S. H. Lu and Y. Liu, *Appl. Catal., B*, 2012, 111–112, 492.
- 19 C. Zhang, W. Lv, Q. H. Yang and Y. Liu, *Appl. Sur. Sci.*, 2012, 258, 7795.
- 20 H. Zhang, D. R. Lin, G. T. Xu, J. B. Zheng, N. W. Zhang, Y. H. Li and B. H. Chen, *Int. J. Hydrogen Energy*, 2015, 40, 1742.
- 21 L. M. Chen, D. Ma, Z. Zhang, Y. Y. Guo, D. Q. Ye and B. C. Huang, *Catal. Lett.*, 2012, 142, 975.
- 22 T. Komatsu, M. Takasaki, K. Ozawa, S. Furukawa and A. Muramatsu, *J. Phys.*

- Chem. C, 2013, 117, 10483.
- 23 L. M. Chen, D. Ma, Z. Zhang, Y. Y. Guo, D. Q. Ye and B. C. Huang, *ChemCatChem*, 2012, 4, 1960.
  - 24 Y. H. Kim, E. D. Park, H. C. Lee, D. Lee and K. H. Lee, *Catalysis Today* 146 (2009) 253–259. (Pt, Rh, Ru/Al<sub>2</sub>O<sub>3</sub>)
  - 25 I. V. Lightcap, T. H. Kosel and P. V. Kamat, *Nano Lett.*, 2010, 10, 577.
  - 26 P. V. Kamat, *J. Phys. Chem. Lett.*, 2012, 3, 663.
  - 27 A. Mukherji, B. Seger, G. Q. Lu and L. Wang, *ACS Nano*, 2011, 5, 3483.
  - 28 Q. J. Xiang, J. G. Yu and M. Jaroniec, *J. Am. Chem. Soc.*, 2012, 134, 6575.
  - 29 L. M. Chen, D. Ma and X. H. Bao, *J. Phys. Chem. C*, 2007, 111, 2229.
  - 30 L. M. Chen, D. Ma, X. Y. Li and X.H. Bao, *Catal. Lett.*, 2006, 111, 133.
  - 31 B. W. Zhong, H. Y. Liu and X. M. Gu, *ChemCatChem*, 2014, 6, 1553.
  - 32 S. Kundu, Y. M. Wang, W. Xia and M. Muhler, *J. Phys. Chem. C*, 2008, 112, 16869.
  - 33 Z. L. Fan, W. Chen, X. L. Pan and X. H. Bao, *Catal. Today*, 2009, 147, 86.
  - 34 L. Perini, C. Durante and M. Favaro, *Appl. Catal., B*, 2014, 144, 300.
  - 35 D. Sebastian, I. Suelves, R. Moliner and M.J. Lazaro, *Carbon*, 2010, 48, 4421.
  - 36 W. X. Huang, X. H. Bao, H. H. Rotermund and G. Ertl, *J. Phys. Chem. B*, 2002, 106, 5645.
  - 37 G. K. Ramesha, J. F. Brennecke and P. V. Kamat, *ACS Catal.* 2014, 4, 3249.
  - 38 J. Deng, P. J. Ren, D. H. Deng, L. Yu, F. Yang and X. H. Bao, *Energy Environ. Sci.*, 2014, 7, 1919.
  - 39 D. H. Deng, L. Yu, X. Chen, G. X. Wang, L. Jin, X. L. Pan, J. Deng, G. Q. Sun and X. H. Bao, *Angew. Chem., Int. Ed.*, 2013, 52, 371.
  - 40 W. J. Zhou, J. Zhou, Y. C. Zhou, J. Lu, K. Zhou, L. J. Yang, Z. H. Tang, L. G. Li and S. W. Chen, *Chem. Mater.*, 2015, 27, 2026.

### Figure Captions

**Fig. 1** Variation of O<sub>2</sub> conversion (A), CO conversion (B), and selectivity (C) over different carbon supported 3 wt.% Pt as a function of the reaction temperature.

**Fig. 2** Variation of O<sub>2</sub> conversion (A), CO conversion (B), and selectivity (C) at 23 °C over different carbon supported Fe and Ni promoted Pt catalysts as a function of the reaction time.

**Fig. 3** TEM images (left) and particle size distribution (right) of different carbon supported Fe and Ni promoted Pt catalysts after activation in H<sub>2</sub> at 500 °C for 2 h. (A) AC; (B) CB-o; (C) CB, and (D) CNTs.

**Fig. 4** The mean particle sizes and catalytic activities of Fe and Ni promoted Pt catalysts at 23 °C as a function of different carbon supports.

**Fig. 5** XRD patterns of carbon supports (A) CNTs, (B) CB, (C) CB-o, (D) AC.

**Fig. 6** The resistivity of supports and catalytic activities of Fe and Ni promoted Pt catalysts at 23 °C as a function of different carbons.

**Fig. 7** Schematic representation of CO oxidation process on the PtFeNi catalysts tuned by the ability of graphitic carbon to capture and shuttle electrons from noble metal to FeO<sub>x</sub>/NiO<sub>y</sub> species through  $\pi$ - $\pi$  network.

**Fig. 8** Variation of O<sub>2</sub> conversion (A), CO conversion (B), and selectivity (C) at 23 °C over CB supported Fe and Ni promoted Pt catalysts as a function of the reaction time.

### Table Captions

**Table 1** The pore texture parameters and the integration area of CO and CO<sub>2</sub> desorption from TPD.

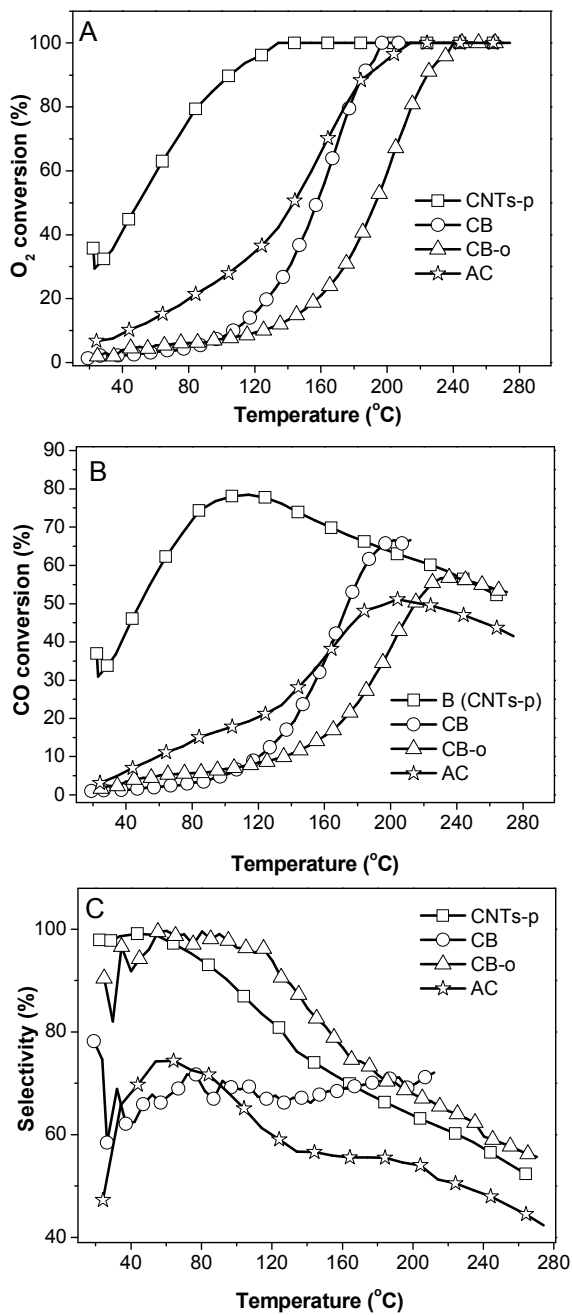


**Fig. 1** Variation of O<sub>2</sub> conversion (A), CO conversion (B), and selectivity (C) over different carbon supported 3 wt.% Pt as a function of the reaction temperature.

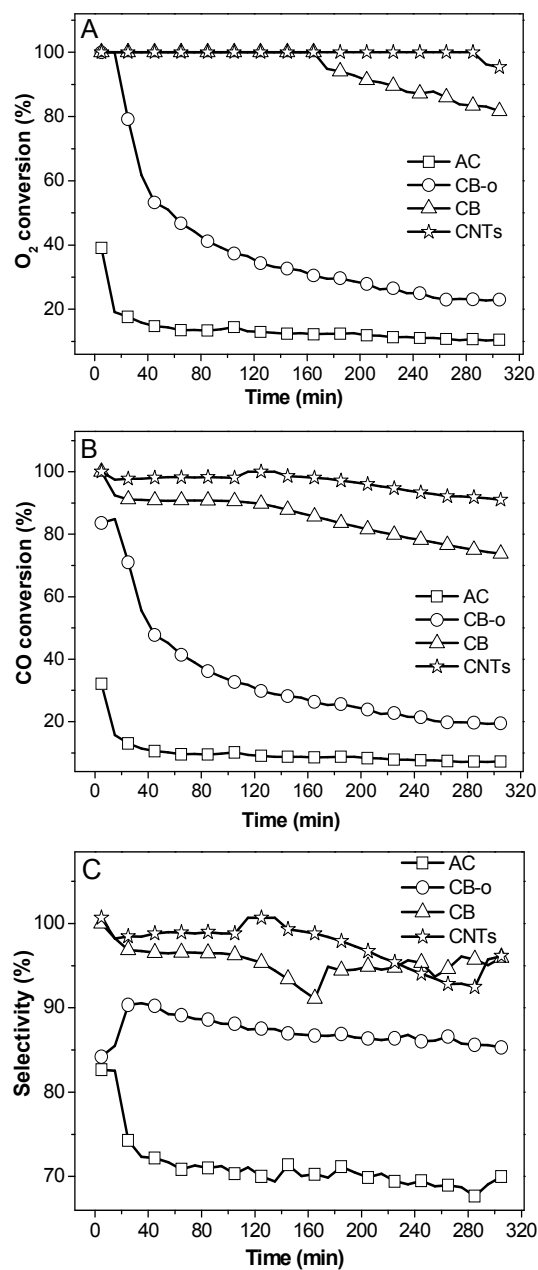


**Fig. 2** Variation of O<sub>2</sub> conversion (A), CO conversion (B), and selectivity (C) at 23 °C over different carbon supported Fe and Ni promoted Pt catalysts as a function of the reaction time.

**Table 1**

The pore texture parameters and the integration area of CO and CO<sub>2</sub> desorption from TPD

Sample	Surface area (m <sup>2</sup> /g)	Mean pore size (nm)	CO <sup>a</sup>	CO <sub>2</sub> <sup>a</sup>	Total <sup>a,b</sup>
AC	1158.0	2.1	4.08	0.49	4.57
CB-O	210.2	11.2	1.35	0.25	1.60
CB	75.8	6.5	0.04	0.03	0.07
CNTs	172.2		0.74	0.17	0.91

<sup>a</sup>Unit: x 10<sup>-7</sup>

<sup>b</sup>the total amounts of released CO and CO<sub>2</sub>

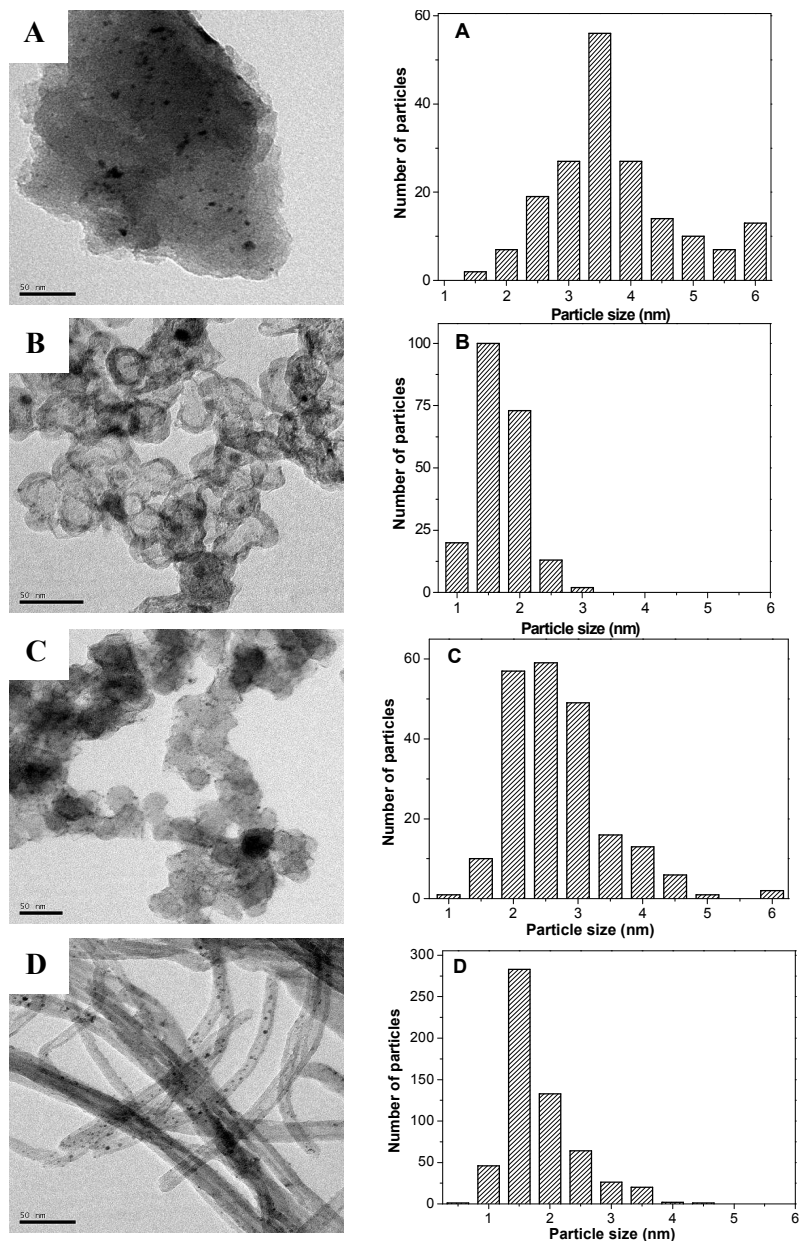


**Fig. 3** TEM images (left) and particle size distribution (right) of different carbon supported Fe and Ni promoted Pt catalysts after activation in  $H_2$  at  $500\text{ }^\circ\text{C}$  for 2 h. (A) AC; (B) CB-o; (C) CB, and (D) CNTs.

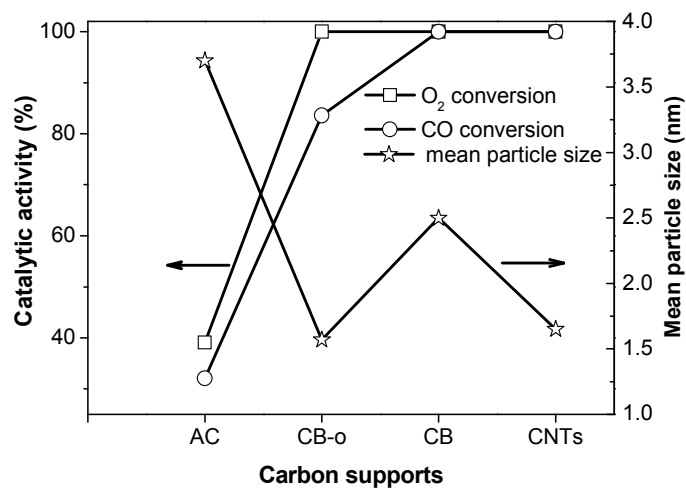


**Fig. 4** The mean particle sizes and catalytic activities of Fe and Ni promoted Pt catalysts at 23 °C as a function of different carbon supports.

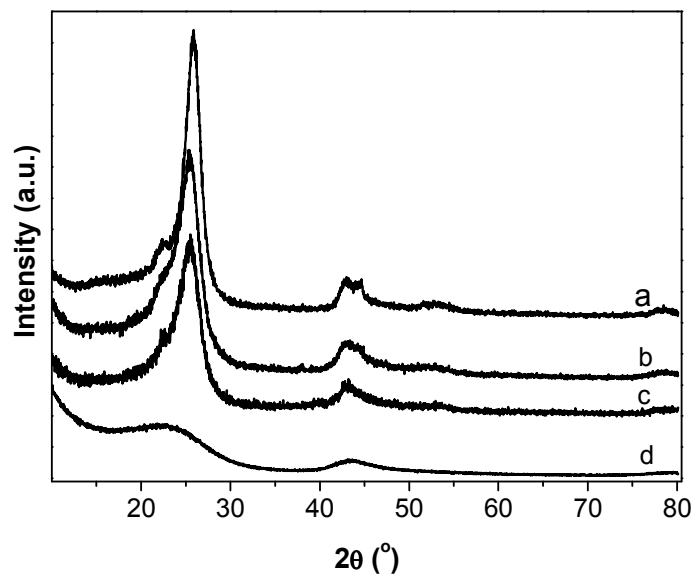


**Fig. 5** XRD patterns of carbon supports (a) CNTs, (b) CB, (c) CB-o, (d) AC.

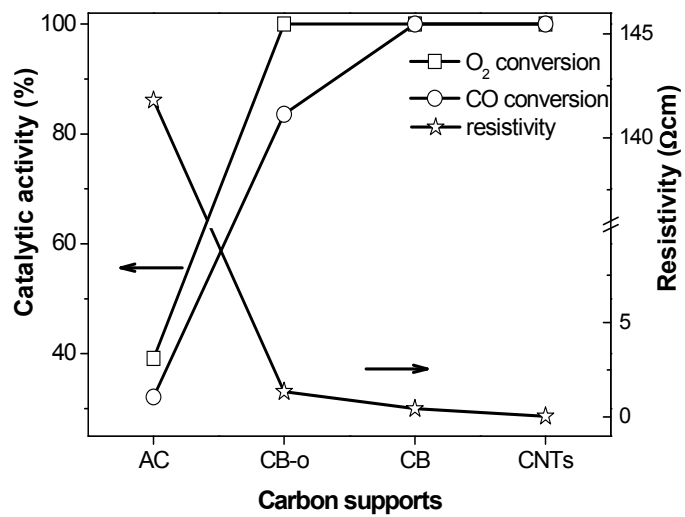


**Fig. 6** The resistivity of supports and catalytic activities of Fe and Ni promoted Pt catalysts at 23 °C as a function of different carbons.

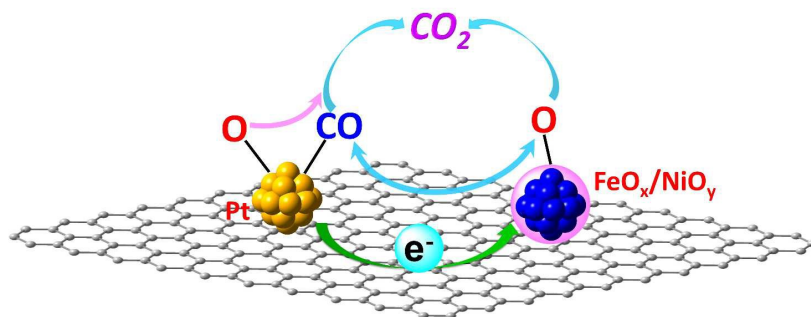


**Fig. 7** Schematic representation of CO oxidation process on the PtFeNi catalysts tuned by the ability of graphitic carbon to capture and shuttle electrons from noble metal to FeO<sub>x</sub>/NiO<sub>y</sub> species through the  $\pi$ - $\pi$  network.

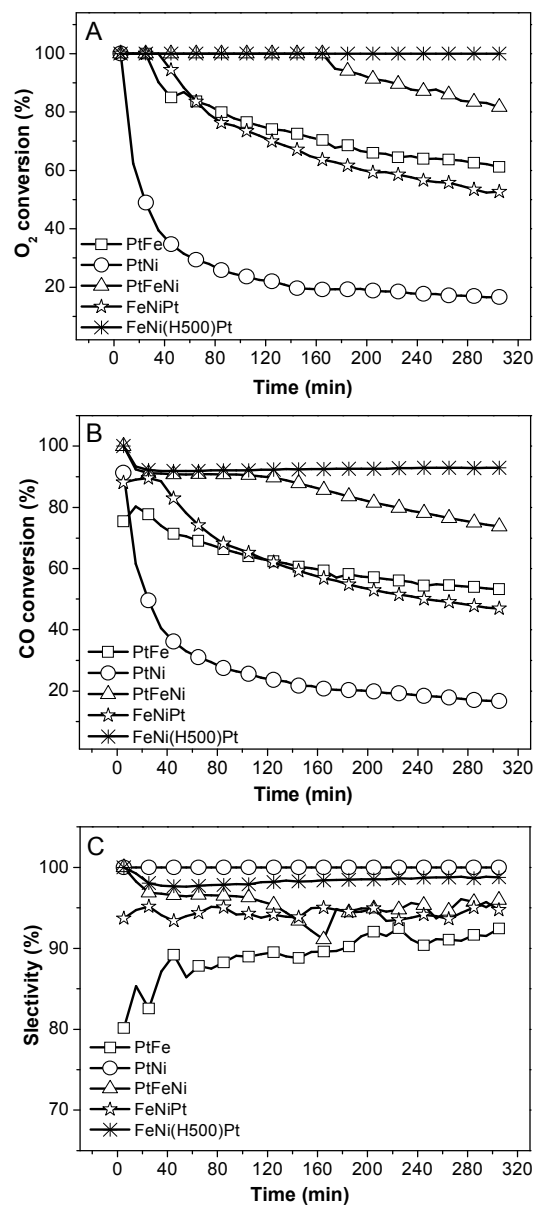
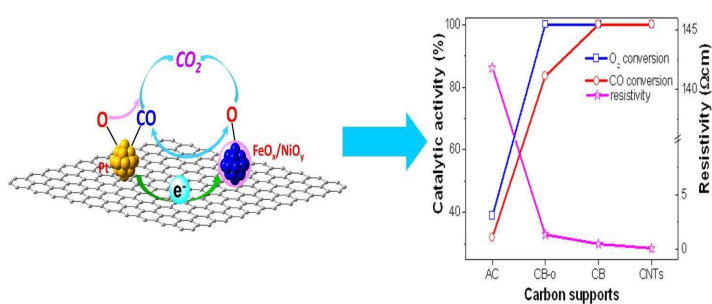


**Fig. 8** Variation of O<sub>2</sub> conversion (A), CO conversion (B), and selectivity (C) at 23 °C over CB supported Fe and Ni promoted Pt catalysts as a function of the reaction time.

## The Graphitic Carbon Strengthened Synergetic Effect between Pt and FeNi for CO Preferential Oxidation in Excess Hydrogen at Low Temperature

Limin Chen<sup>a,b\*</sup>, Yunfeng Bao<sup>a</sup>, Yuhai Sun<sup>a</sup>, Ding Ma<sup>b,c</sup>, Daiqi Ye<sup>a</sup>, Bichun Huang<sup>a</sup>



### Highlights

The extremely good catalytic performance of PtFeNi/CNTs catalyst at low temperature with relatively low Pt loading is due to the graphitic carbon strengthened synergetic effect between Pt and FeNi.